

# Coupling the Level Set Method with an electro-thermal solver to simulate GST based PCM cells

A.Glière, O.Cueto, J.Hazart  
CEA, LETI, MINATEC Campus  
F-38054 Grenoble, France  
e-mail: olga.cueto@cea.fr

**Abstract**—The Level Set Method and a GST thermodynamic model are coupled to an electrothermal solver to simulate GST based PCM cells. A good qualitative agreement with published results is obtained in the cell amorphization simulation and the ability of our method to simulate crystallization is demonstrated.

*PCM Simulation; Level Set Method; Crystallization*

## I. INTRODUCTION

Phase Change Memory (PCM) is an emerging technology for non-volatile memory devices. Expected benefits are high speed, single bit writing granularity, potential scalability to the 10 nm technology node, long cycle life and good compatibility with standard CMOS fabrication processes. The device's operation relies on reversible and fast switching between the amorphous and crystalline phases of chalcogenide materials, such as  $\text{Ge}_2\text{Sb}_2\text{Te}_5$  (GST). At room temperature, the two phases exhibit very different conductivities and this contrast is used to establish the memory effect.

In this paper, the coupling of the Level Set Method (LSM) and a GST thermodynamic model to an electrothermal solver is presented and the model ability to simulate both phase transitions in GST based PCM is demonstrated.

## II. PRESENTATION OF THE LEVEL SET METHOD

### A. Main Features of the Level Set Method

The LSM has been successfully used in applications involving the motion of complex interfaces [1][2], such as the one under consideration, separating crystal and amorphous phases during nucleation and growth. Using the LSM, the interface  $\Gamma$  between two domains is captured as the zero level set of a smooth function  $\varphi$ :

$$\Gamma(t) = \{(x,t) \mid \varphi(x,t) = 0\}. \quad (1)$$

The interface transient motion is computed by advecting the level set function  $\varphi$  with a velocity field  $\mathbf{v}$ , defined by the physical problem to solve:

$$\partial\varphi/\partial t + \mathbf{v} \cdot \mathbf{grad} \varphi = 0. \quad (2)$$

The distinctive advantages of the LSM, which belongs to the “front capturing” methods category, are (i) its intrinsic ability to deal with multiply connected interfaces and their topological changes as phases merging and breaking do not need any extra effort, (ii) its natural extension to three-dimensional problems and (iii) its capability to provide accurate values of the interface normal and curvature.

In this work,  $\Gamma$  lies between the crystal and amorphous phases and the interface velocity is the crystal growth speed. The chosen level set function is defined as a signed distance, positive in the crystal phase and negative in the amorphous phase.

### B. Simulation of Nucleation and Growth

The crystallization of phase change material occurs in two steps, namely crystal nucleation and growth of the crystal phase. A thermodynamic approach is considered [3][4], which takes into account both homogeneous nucleation, occurring in the bulk of the GST material, and heterogeneous nucleation, present around impurities and at the external boundaries of the GST material. Only the heterogeneous nucleation, which is largely prevalent in our configuration, is described in details hereunder. However, homogeneous nucleation is treated in a quite similar manner.

#### 1) Crystal nucleation

Due to the very fast increase (in the order of  $10^{12}$  K/s) and decrease of temperature (in the order of  $10^{10}$  K/s) associated to the electrical pulses used in PCM, a transient nucleation rate is taken into account [4] through the equation

$$I = I_s \exp(-\tau/\delta t), \quad (3)$$

in which  $\tau$  is the time needed to establish the stationary state population of nuclei and  $\delta t$  is the isothermal holding time, based on the local temperature variation rate  $\partial T/\partial t$ . The stationary nucleation rate  $I_s$  is defined by:

$$I_s = N \gamma O_n Z_c \exp(-\Delta G^*/(kT)). \quad (4)$$

In the latter equation,  $N$  is the density of nucleation sites (or the atomic density in the case of homogeneous nucleation),  $\gamma$  is the atomic jump frequency,  $O_n$  is the number of atoms at the

surface of the critical size nucleus,  $Z_c$  is the Zeldovich factor,  $\Delta G^*$  is the free energy associated to the creation of a stable nucleus and  $k$  is the Boltzmann constant.

The atomic jump frequency is calculated with the Stokes-Einstein law

$$\gamma = k T / (2.4 \eta d^3), \quad (5)$$

involving the viscosity  $\eta$  and the interatomic distance  $d$ . The material viscosity is a function of temperature and the viscosity law depends on the melting temperature  $T_m$  and the glass transition temperature  $T_g$ .

The Zeldovich factor for GST material is defined by

$$Z_c = (\Delta G_v / (6\pi R T n^*) M / 9\rho)^{1/2}, \quad (6)$$

where  $\Delta G_v$  is the difference between the Gibbs free energy per unit volume of the amorphous and crystalline phase,  $R$  the gas constant,  $n^*$  the number of atoms in the critical size nucleus,  $M$  the molar mass and  $\rho$  the material density.  $\Delta G_v$  is calculated with the relation provided by Thompson and Spaepen [5]

$$\Delta G_v = (L_m / T_m) T \ln(T_m / T), \quad (7)$$

where  $L_m$  is the latent heat of melting.

Finally, the free energy  $\Delta G^*$  for the creation of a stable nucleus by heterogeneous nucleation is calculated using the expression

$$\Delta G^* = 4 (\chi + 5 \sigma_{ac})^3 / (27 \Delta G_v^2), \quad (8)$$

where  $\chi$  is the surface energy, describing the chemical affinity between the phase change material and the surrounding materials, and  $\sigma_{ac}$  is the interfacial energy per unit area between the crystalline nucleus and the amorphous phase matrix.

The numerical values of the GST thermodynamical parameters involved in the crystal nucleation model are listed in Table 1.

TABLE I. VALUES OF GST THERMODYNAMICAL MODEL PARAMETERS.

Parameter	Value	Definition
$N$	$10^{23} \text{ m}^{-3}$	density of nucleation sites
$d$	$3 \cdot 10^{-10} \text{ m}$	interatomic distance
$\rho$	$6150 \text{ kg/m}^3$	density
$M$	$1.026 \text{ kg/mol}$	molar mass
$L_m$	$11.2 \cdot 10^8 \text{ J/m}^3$	latent heat of melting
$T_m$	$880 \text{ K}$	melting temperature $T_m$
$T_g$	$353 \text{ K}$	glass transition temperature
$\chi$	$-0.3 \text{ J/m}^2$	chemical affinity surface energy
$\sigma_{ac}$	$0.1 \text{ J/m}^2$	crystal-amorphous interfacial energy

## 2) Growth of the Crystal Phase

Classically [4], the crystal growth speed, used to evolve the crystalline area interface, is given by:

$$v = \gamma d [1 - \exp(-\Delta G_v M / (9\rho RT))]. \quad (9)$$

## III. COUPLING THE LEVEL SET METHOD WITH AN ELECTROTHERMAL SOLVER

### A. Electrothermal Solver

Threshold switching is the essential mechanism involved in the PCM devices set transition. Several modeling possibilities have been explored to date but the nature of the switching mechanism remains controversial. Among others, Kim et al. [6] and David Wright et al. [7] used an ohmic model approach based on the current conservation equation, Redaelli et al. [8] placed themselves in the semiconductor modeling framework and used the drift-diffusion equations for electrons and holes, Ielmini and Zhang [9] developed an analytical model based on a Poole-Frenkel conduction mechanism and Karpov et al. [10] provided evidences in favor of a field-induced nucleation model.

In this paper, an approach similar to that of David Wright et al. [7] is retained to simulate the electrical behavior of the PCM cell. The electrothermal solver, used to determine the distributions of electric potential  $V$ , electric current density  $\mathbf{j}$  and temperature  $T$ , thus relies on the coupled system of partial differential equations formed by the current conservation equation (10) and the heat transfer equation (11):

$$\text{div}(-\sigma \text{ grad } V) = 0, \quad (10)$$

$$\rho C_p \partial T / \partial t - \text{div}(-k \text{ grad } T) = \mathbf{j}^2 / \sigma, \quad (11)$$

where  $\sigma$ ,  $\rho$ ,  $C_p$  and  $k$  respectively stand for the materials electrical conductivity, density, heat capacity and thermal conductivity.

The associated boundary conditions depend on the cell configuration. They are either Dirichlet (fixed electric potential on the cell electrodes and fixed room temperature) or Neumann (electrical and thermal insulation).

The simulation of the threshold switching mechanism is based on the electric field dependence of the amorphous GST conductivity [7]. Moreover, both crystalline and amorphous GST conductivities are temperature dependant. They are given by the expressions:

$$\sigma_{cr} = \sigma_{cr}^0 \exp(-E_{cr} / (kT)), \quad (12)$$

$$\sigma_{am} = \sigma_{am}^0 \exp(-E_{am} / (kT)) \exp(E / E_0), \quad (13)$$

where  $\sigma_{cr}^0$  and  $\sigma_{am}^0$  are prefactors for the conductivities of crystalline and amorphous GST,  $E_{cr}$  and  $E_{am}$  are the thermal

activation energies and  $E_0$  is the critical electric field for switching.

In order to avoid the occurrence of non realistic temperatures in the PCM cell, a phase and temperature dependent thermal conductivity in GST is used. Data from Rajendran et al. [11] are plotted in Fig. 1.

The numerical values of the GST parameters needed in (12) and (13) are listed in Table 2. The other materials electrical conductivity, density, heat capacity and thermal conductivity are commonly accepted values excerpted from the literature or have been measured at CEA-LETI facilities (Table 3).

### B. Numerical Methods and Implementation

The current conservation and heat transfer equations are spatially discretized in two-dimensions by the Finite Volume Method. The meshing algorithm creates an adaptive quadtree grid which can be locally refined, for example in the GST material domain.

The solver deals with the strong coupling of the thermal and electrical problems as well as the highly non linear behavior of the problem. The latter is due to the exponential dependence of the electrical conductivities of both GST phases to temperature and to the exponential dependence of the electrical conductivity of the amorphous phase to the electric field. The solution of the non linear transient system is carried out by two nested fixed point algorithms, respectively for electric potential and temperature, embedded in a semi-implicit Crank-Nicolson adaptive time scheme. Depending on user requirements, this time scheme can be made totally implicit.

The LSM, which manages the phase evolution in the GST material is coupled explicitly to the preceding system and includes the following computational steps: (i) calculation of local homogeneous and heterogeneous nucleation rates and crystal growth speed, (ii) random nucleation in the amorphous material, (iii) transient evolution of the level set function according to (2) and (iv) segmentation of the GST domain in three different phases (crystal, amorphous and liquid above fusion temperature).

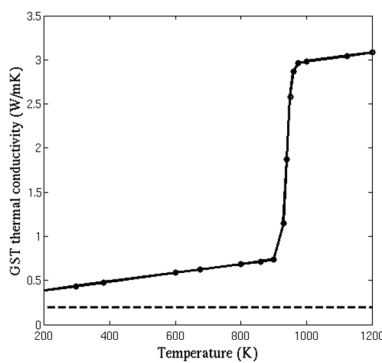


Figure 1. Thermal conductivity for crystalline/melted (solid line) and amorphous GST (dashed line).

TABLE II. VALUES OF GST CONDUCTIVITY MODEL PARAMETERS.

Parameter	$\sigma_{cr}^0$	$E_{cr}$	
Value	$2 \cdot 10^4$ S/m	0.039 eV	
Parameter	$\sigma_{am}^0$	$E_{am}$	$E_0$
Value	$2 \cdot 10^5$ S/m	0.34 eV	$5 \cdot 10^7$ V/m

TABLE III. VALUES OF THE ELECTRICAL AND THERMAL PARAMETERS.

Material	$\sigma$ (S/m)	$\rho$ (kg/m <sup>3</sup> )	$C_p$ (Jm <sup>-3</sup> K <sup>-1</sup> )	$k$ (Wm <sup>-1</sup> K <sup>-1</sup> )
Cu	$5.8 \cdot 10^7$	8900	385	401
TiN	$1.22 \cdot 10^6$	5430	784	19.2
GST	(12) and (13)	6150	210	Fig. 1
SiO <sub>2</sub>	$10^{-14}$	2330	1330	1.4
Al	$3.77 \cdot 10^7$	2700	900	240

The level set function is computed on a regular mesh, built on the GST domain only. In the second computational step described above, the stochastic character of nucleation is reproduced as follows: in each LSM mesh cell of the PCM domain, if the temperature is below the melting temperature and the cell is not in the crystalline phase, a Monte Carlo approach of nucleation is used, where the nucleation probability is defined from the local nucleation rates.

On user's request, the external circuit driving the PCM can be represented by an additional ordinary differential equation, coupled to the solver and providing the value of the bias applied between the cell's electrodes.

The method is implemented in a versatile software, built on Matlab. The software addresses various situations as it accommodates two-dimensional Cartesian and axisymmetrical geometries and incorporates user defined functions dedicated to geometry description, physical properties and boundary conditions. Computational speed-up is obtained by coding a few critical functions in C language.

## IV. APPLICATIONS AND DISCUSSIONS

First, the simulation of an amorphization pulse applied to a confined type PCM cell, initially placed in fully crystalline state, is presented. The simulation is carried out in axisymmetrical coordinates on a confined type structure represented by Fig. 2. The external driving circuit comprises a load resistance (170  $\Omega$ ) and an external capacitance ( $10^{-11}$  F). Several distinct amorphization pulses are generated (inset of Fig. 3) whose maximum value varies between 0.5 V and 3 V. The programming current is defined as the maximum of the current through the PCM cell during each amorphization pulse. The low field resistance is obtained by applying a low voltage pulse (0.1 V) to the PCM cell after the amorphization pulse, once the temperature has returned to close to ambient values. The low field resistance versus programming current is plotted in Fig. 3, showing that our amorphization simulation is in good qualitative agreement with that of Kim et al. [6]. Moreover, the model accuracy could be improved by implementing a correction factor accounting for space averaging in the azimuthal direction (in axisymmetrical geometries, each crystal or amorphous element in the ( $\rho$ ,  $z$ ) plane represents a complete ring in the azimuthal direction).

The ability of the method to simulate crystallization is also demonstrated as follows. The cell phase state obtained after an

amorphization pulse is used as initial conditions for a set pulse (rise and fall times: 3 ns, pulse width: 100 ns, pulse: 1.8 V). When the temperature in the GST domain reaches the temperature range where nucleation is highly probable (540 to 673 K), the simulation shows nucleation and growth of the crystal phase, finally leading to partial crystallization of the amorphous domain (Fig. 4). Let us note that, as expected, the homogeneous nucleation rate is several orders of magnitude smaller than the heterogeneous nucleation rate and could be safely neglected.

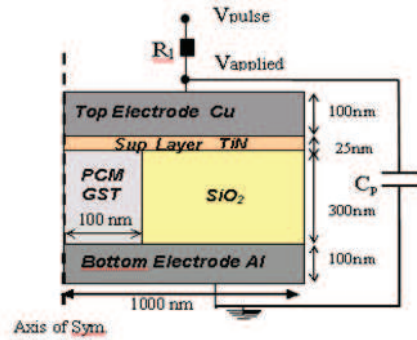


Figure 2. Simulation setup for the confined type PCM cell.

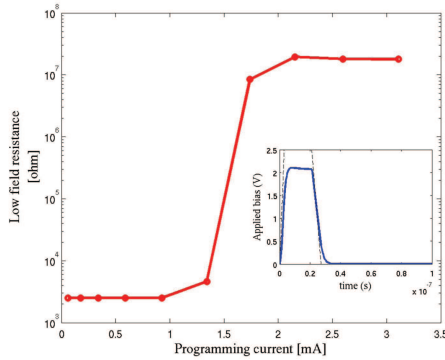


Figure 3. Low field resistance as a function of programming current. The inset shows the 2.5 V amorphization pulse (dashed line) and the bias applied to the cell (solid line).

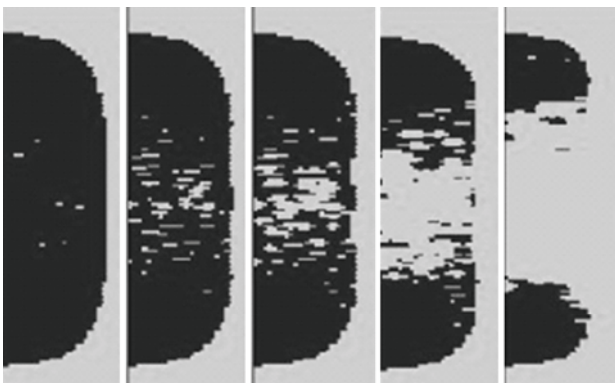


Figure 4. Close up view of the GST domain. From left to right : melted-quenched initial conditions, nucleation and growth of the crystal phase at  $75 \cdot 10^{-9}$ s,  $80 \cdot 10^{-9}$ s, and  $90 \cdot 10^{-9}$ s, recrystallized sample after  $95 \cdot 10^{-9}$  s. The crystal phase is shown in grey and the amorphous phase in black.

## V. CONCLUSION

This paper presents the coupling of the LSM and a GST thermodynamic model with an electrothermal solver to simulate phase change dynamics in PCM cells. To our knowledge, the LSM had not been applied to PCM simulation before this work. The model implementation addresses the main simulation issues faced by the PCM cells designers, namely both phase transitions and data retention. A good qualitative agreement with published work is obtained in the amorphization simulation [6] and the ability of our method to simulate crystallization is demonstrated.

Comparisons with electrical results on PCM cells fabricated in our clean-room facilities, including a complete calibration of electrical and thermal properties of the materials, are ongoing. The LSM ability to naturally extend to the third dimension will facilitate the extension of the solver to the simulation of three-dimensional problems. Due to its versatility, an extension of the LSM based software to the simulation of other kinds of resistive memories (OxRAM and CBRAM) is also considered.

## ACKNOWLEDGMENT

The authors thank V. Sousa, L. Perniola and B. Hyot from CEA-LETI for fruitful discussion. They also acknowledge the development work carried out on the quadtree meshing software by F. Huguet, now with ST Microelectronics.

## REFERENCES

- [1] S. Osher and R. Fedkiw, "Level Set Methods: An overview and Some Recent Results," *J. Comp. Phys.*, vol. 169, no. 2, 2001.
- [2] F. Gibou, R. Fedkiw, R. Caflisch and S. Osher, "A Level Set Approach for the Numerical Simulation of Dendritic Growth," *J. Sci. Comput.*, vol. 19, pp. 183-199, 2003.
- [3] K.F Kelton, A.L Greer and C.V. Thompson, "Transient Nucleation in condensed systems," *J. Chem. Phys.*, vol. 79, no. 12, 1983.
- [4] B. Hyot, L.Poupinet, V.Gehanno and P.J Desre, "Analysis of writing and erasing behaviours in phase change materials," *J. Magn. Magn. Mater.*, vol. 249, pp. 504-508, 2002.
- [5] C.V. Thompson and F. Spaepen, "On the approximation of the free energy change on crystallization," *Acta Metallurgica*, vol. 27, pp. 1855-1859, 1979.
- [6] D.H. Kim, F.Merget, M.Först, H.Kurz, "Three-dimensional simulation model of switching dynamics in phase change random access memory cells," *J. Appl. Phys.*, vol. 101, 2007
- [7] C. David Wright, M.Armand and M.M. Aziz, "Terabit-per-square-inch data storage using phase-change media and scanning electrical nanopores," *IEEE Trans. Nanotechnol.*, vol. 5, no. 1, p. 50, 2006.
- [8] A. Redaelli, A. Pirovano, A. Benvenuti, et A. L. Lacaita, "Threshold switching and phase transition numerical models for phase change memory simulations", *J. Appl. Phys.*, vol. 103, no. 11, 2008.
- [9] D. Ielmini et Y. Zhang, "Analytical model for subthreshold conduction and threshold switching in chalcogenide-based memory devices", *J. Appl. Phys.*, vol. 102, no. 5, p. 054517, 2007.
- [10] I. V. Karpov, M. Mitra, D. Kau, G. Spadini, Y. A. Kryukov, et V. G. Karpov, "Evidence of field induced nucleation in phase change memory", *Appl. Phys. Lett.*, vol. 92, no. 17, p. 173501, 2008.
- [11] B. Rajendran, J. Karidis, M-H. Lee, M. Breitwisch, G.W. Burr, Y-H. Shih, et al., "Analytical Model for RESET operation of Phase Change Memory," *IEDM Technical Digest* vol. 1, pp. 5-22, 2008.